ACS Catalysis

Research Article

pubs.acs.org/acscatalysis

Selectivity in Propene Dehydrogenation on Pt and Pt_3Sn Surfaces from First Principles

Lauri Nykänen[†] and Karoliina Honkala*

Department of Chemistry, Nanoscience Center, University of Jyväskylä, P.O. Box 35, FIN-40014 Jyväskylä, Finland

Supporting Information

ABSTRACT: Propene can be produced via dehydrogenation of propane on Pt-based catalysts; however, the catalysts are plagued by low selectivity toward propene and high coke formation. The selectivity can be improved and the coke formation reduced by alloying Pt with Sn. The alloying is known to weaken the binding of propene, which in part explains the improved performance. We conducted density functional theory calculations to study the dehydrogenation of propene on flat and stepped Pt and Pt_3Sn surfaces. The steps on Pt dehydrogenate propene readily, whereas, on Pt_3Sn, the steps are inert because they are decorated with Sn. Our results indicate that the high selectivity and low coking on the Pt−Sn catalyst can result from a lack of active Pt step sites.

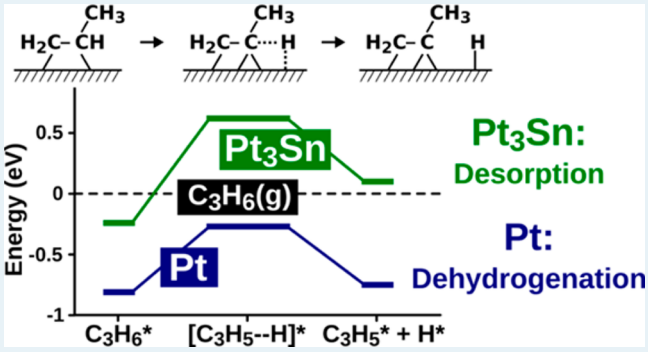

KEYWORDS: *heterogenous catalysis, selectivity, propene dehydrogenation, density functional theory, Pt, Pt_3Sn alloy, atomistic thermodynamics*

INTRODUCTION

Propene is a valuable raw material that is used for making, for example, plastics, paints, and medicines.[1,2] It is mostly produced as a byproduct of other processes, but the growing need for propene has prompted research and development of on-purpose production technologies. An appealing propene synthesis method is dehydrogenation of propane (DHP) in the presence of a catalyst.[3] In particular, Pt particles are used to catalyze dehydrogenation reactions, but they deactivate fast as a result of coke formation.[4,5] The performance of a Pt catalyst can be improved via modifying its properties with Sn.[6] The addition of Sn is especially observed to weaken propene adsorption[7,8] and improve the selectivity of DHP on Pt catalyst.[6] Furthermore, Sn is also suggested to reduce coke formation over the catalyst particles, the main benefits of which are slower deactivation and less frequent regeneration of a catalyst. Usually, propane dehydrogenation is done at relatively high temperature, 770−900 K, to make the reaction thermodynamically feasible.[9]

A crucial point in the DHP reaction is what happens to propene once it is formed on a catalyst surface. According to temperature-programmed desorption (TPD) and spectroscopic experiments, propene dehydrogenation to propylidyne takes place between 230 and 270 K on Pt(111), depending on the initial propene coverage and desorption temperature,[7,10,11] whereas desorption has been determined to take place at ∼280 K on Pt(111).[7,11,12] Propene adsorption properties display similarities to ethylene properties, including the same adsorption temperature and the most favorable adsorption geometry, di-σ. For ethylene adsorption and dehydrogenation, the central role of low-coordinated metal sites is well established from experiments and computations.[13−15] This raises the question whether the low-coordinated sites have a central role for DHP on Pt catalysts and, in particular, improved selectivity on Pt−Sn catalysts. Spectroscopic experiments for CO adsorption on Pt−Sn particles show that Sn atoms are located at step edges.[16] The decoration of steps with Sn is also observed to correlate with an improved selectivity in dehydrogenation of ethane to ethene. Previous density-functional-theory (DFT) calculations indicate that low-coordinated sites on Pt(211)[17] and on supported Pt_4 clusters[18] do not introduce competition between C−C and C−H bond-breaking steps at the level of propene, but dehydrogenation is always more favorable. Among the possible reaction steps, desorption of propene is the desired process, whereas dehydrogenation leads to fragments for which a C−C bond rupture can be more favorable, leading to coke formation and catalyst deactivation. Therefore, competition between propene desorption and dehydrogenation should control the DHP selectivity. This so-called thermodynamic selectivity concept has been previously identified for alkyne/alkane mixtures[19] and acetylene hydrogenation.[20] Both TPD measurements and DFT calculations indicate that alloying Pt with Sn weakens propene adsorption.[7,8,21] Experimentally, nearly all propene is observed to desorb, and dehydrogenation is negligible on Pt_3Sn/Pt(111)

Received: July 16, 2013
Revised: November 5, 2013
Published: November 8, 2013

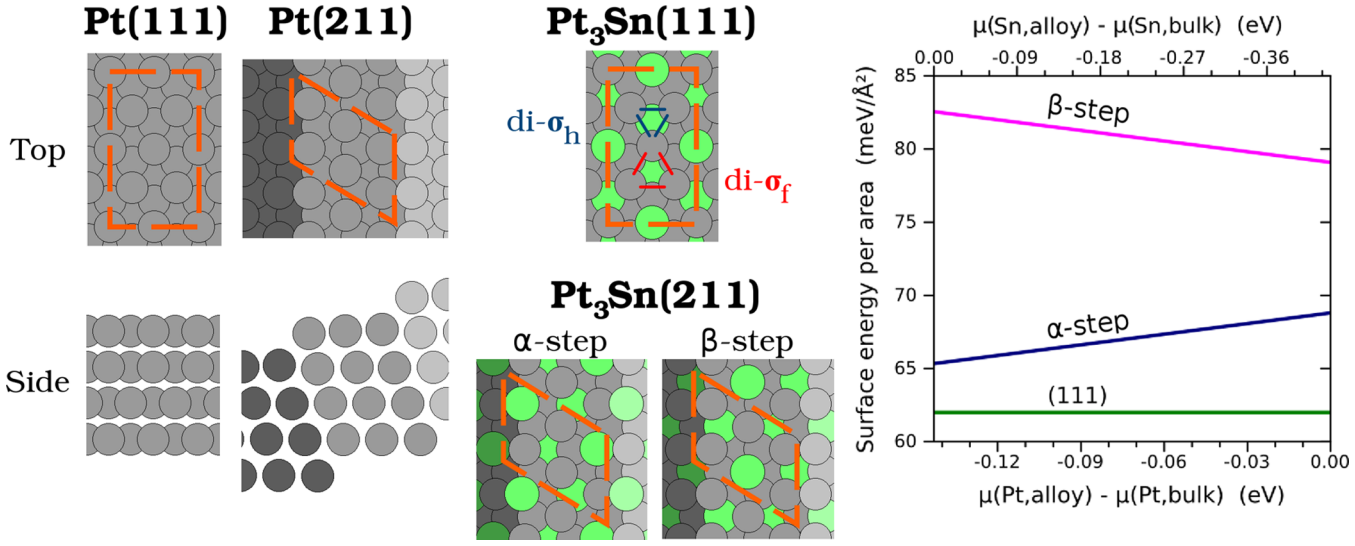

Figure 1. On the left side are the model surfaces used in this study. The surface unit cells are indicated with dashed lines. Spheres representing Pt are gray, and Sn atoms are green. On the (211) surfaces, the higher terraces have a lighter coloring, and lower terraces, a darker coloring. On the right side is a plot of the surface energies of $Pt_3Sn(111)$ and the two $Pt_3Sn(211)$ surfaces: α- and β-step. Only the chemical-potential range at which the alloy is stable is presented.

and $Pt_2Sn/Pt(111)$ surface alloys.[7] On supported PtSn catalysts also, coking is reported.[6]

In this work, we have conducted DFT calculations with the aim to understand the role of low-coordinated sites for improved propene dehydrogenation selectivity on Pt_3Sn. The main focus is in thermodynamic and kinetic factors controlling selectivity, but the details of electronic structure have been thoroughly discussed in earlier studies.[8,17,18,21−23] Our results indicate that although the defect sites on Pt are very reactive, leading deep dehydrogenation of propene, they are passivated by Sn on the alloy surface. This difference in defect-site reactivity might be the factor that sets Pt and Pt−Sn alloys apart.

COMPUTATIONAL METHODS

All calculations were performed with the GPAW program.[24] Exchange and correlation effects were described with a revised Perdew−Burke−Ernzerhof (RPBE) functional,[25] which is known to yield a very good description of adsorption on transition metal surfaces. It has also been successfully used for the study of unsaturated hydrocarbons on Pt and Pt−Sn surface alloys.[26] Transition states were determined using the drag method and validated with vibrational calculations. See the Supporting Information for more details. Slab models were employed to represent flat and stepped Pt (Pt_3Sn) surfaces that stand for terraces and edges of catalyst particles. We chose to model a step surface with the (211) surface because the step edge has the same geometry as steps on a fcc(111) surface. The models employed are sketched in Figure 1. It is possible to create $Pt_3Sn(211)$ in two different ways, as illustrated in Figure 1 and denoted as α- and β-step. The difference between the two stepped alloy surfaces is that in the β model, the step edge has only Pt atoms, whereas in the α model, the step edge contains both Pt and Sn atoms at a ratio of 1:1.

To estimate the relative stability of α- and β-steps of Pt_3Sn, we calculated surface energies using atomistic thermodynamics.[27] For more details, please see the Supporting Information. Figure 1 shows that the α-step is more stable than the β-step at chemical potential values for a stable alloy. This is in agreement with the fact that Sn has lower surface energy than Pt, and it indicates that the majority of the steps on Pt−Sn particles resemble α-type steps. So far, we have assumed that surface composition is equal to bulk composition. This might be a too-simplistic model, particularly on the step edge, where segregation could strongly impact reactivity, reducing a number of Sn atoms at the step edge. To explore this possibility, we have calculated the segregation energy for an α-step without an adsorbate. Two different cases are addressed: a step Sn atom is exchanged with a subsurface Pt atom, and a step Sn atom is exchanged with a terrace Pt atom. The energies are referenced to the bulk-terminated step edge. Subsurface and terrace exchanges are unstable by 2.09 and 0.93 eV, respectively. These segregation energies are too endothermic to be compensated by the adsorption energy of propene, as we will show later.

RESULTS

Consistent with several previous DFT results,[8,18,21−23] propene prefers a di-σ site on Pt(111) with an adsorption energy of −0.51 eV over a π site, which is 0.2 eV less stable. The adsorption energy for a di-σ site agrees reasonably well with desorption activation energy estimated from TPD measurements, for which two different values are given in the literature: 0.52[12] and 0.75 eV.[7]

On $Pt_3Sn(111)$, two different di-σ sites are present, as can be seen from Figure 1. They are called di-σ_f and di-σ_h because they overlap with 3-fold hollow fcc and hcp sites, respectively. On $Pt_3Sn(111)$, propene favors a di-σ_h site with an adsorption energy of −0.24 eV. A similar preference for a di-σ_h site over a di-σ_f site was also reported for ethene adsorption on $Pt_3Sn(111)$.[28] Our propene adsorption energy is somewhat less exothermic than the previously reported value, −0.5 eV, that was obtained employing the PBE functional.[21,29] We found that the two other sites, di-σ_f and π, bind propene ∼0.2 eV more weakly and thus, are nearly thermoneutral. The stronger adsorption on Pt(111) than on $Pt_3Sn(111)$ can be explained with a lowered d-band center of the Pt atoms on $Pt_3Sn(111)$.[8] Because Sn donates electrons to Pt in Pt−Sn alloys, it can also

dx.doi.org/10.1021/cs400566y | ACS Catal. 2013, 3, 3026−3030

contribute to the weaker adsorption as a result of increased Pauli repulsion between propene π and Pt d electrons.[30]

On Pt(211), propene favors a di-σ site along the step edge of Pt(211) with the methyl group pointing away from the terrace (see Figure 2d), in agreement with a previous DFT study.[17]

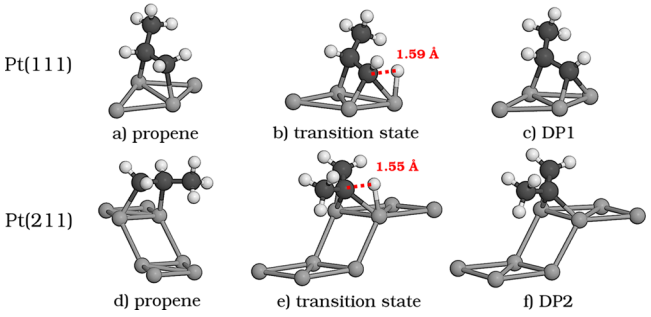

Figure 2. Adsorption geometries of the (a, d) initial, (c, f) final, and (b, e) transition states of propene dehydrogenation. The spheres represent atoms: hydrogen, white; platinum, light gray; and carbon, dark gray. The red dotted lines highlight the breaking bonds, and the bond length at the transition state is given.

Compared with Pt(111), adsorption becomes more exothermic, with an adsorption energy of −0.81 eV. A higher reactivity of step atoms is manifested as stronger binding of propene to the low-coordinated step atoms that have a higher d-band center compared with the flat surface.[31] The α-step binds propene weakly, with adsorption energies of −0.15 and −0.01 eV for di-σ_f and di-σ_h sites, respectively. The slight favoring of the di-σ_f site originates from the fact that the site is at the step edge (see Figure S3d), unlike the di-σ_h site, where propene is sterically hindered by the upper-terrace atoms (Figure S3g). On the β-step, propene adsorption energy on a di-σ_h site is close to the value on Pt(211): −0.75 eV (see Figure S3j). This indicates that propene adsorption energy is dominated by the reactivity of the active site, and the impact of the neighboring atoms is minor. A weakening of propene adsorption promotes desorption, and this happens with an increasing concentration of Sn.[8] Eventually, the decreased Pt content might affect propane dehydrogenation and reduce propene formation. Thus, a PtSn catalyst is a compromise: it must efficiently convert propane to propene, but it must not dehydrogenate propene.

Next, a crucial step to selectivity, propene dehydrogenation to C_3H_5, is addressed. We start by discussing the adsorption properties of the dehydrogenation products. The adsorption energies are given with respect to gas phase propene. Propene has three direct dehydrogenation products, namely, propan-2-yl-1-ylidene (DP1), propan-1-yl-2-ylidene (DP2), and 1,2,3-propanetriyl (DP3), and their chemical formulas are $CHCHCH_3$, CH_2CCH_3, and CH_2CHCH_2, respectively (see Figure S2 in the SI). DP1 and DP2 are formed when a H atom is removed from one of the C atoms bound to the surface, whereas methyl group dehydrogenation produces DP3. On Pt(111), DP1 and DP2 adsorb on 3-fold hollow sites (see Figure S1c and d in the SI) with an adsorption energy of ∼−0.4 eV. On $Pt_3Sn(111)$, adsorption becomes weaker, and adsorption energies are ∼−0.1 and ∼0.4 eV on hcp and fcc sites, respectively. Again, this agrees well with the results of Watwe et al., who reported a strong preference to a hcp over a fcc site for CCH_3 on $Pt_3Sn(111)$.[28] DP3 prefers a di-σ/π mode on the flat surfaces, with one C−C bond coordinated to one Pt atom and the other to two Pt atoms (see SI Figure S1e). The adsorption energy for DP3 is −0.5 eV (−0.26 eV) on a Pt(111) ($Pt_3Sn(111)$) surface. Similar to propene adsorption, low-coordinated atoms enhance the DPs' adsorption considerably on Pt(211), whereas adsorption becomes endothermic on an α-step of $Pt_3Sn(211)$ because the step edge consists of the weakly binding fcc sites, and at the hcp sites, the DPs are sterically hindered (see Table S3 in the SI).

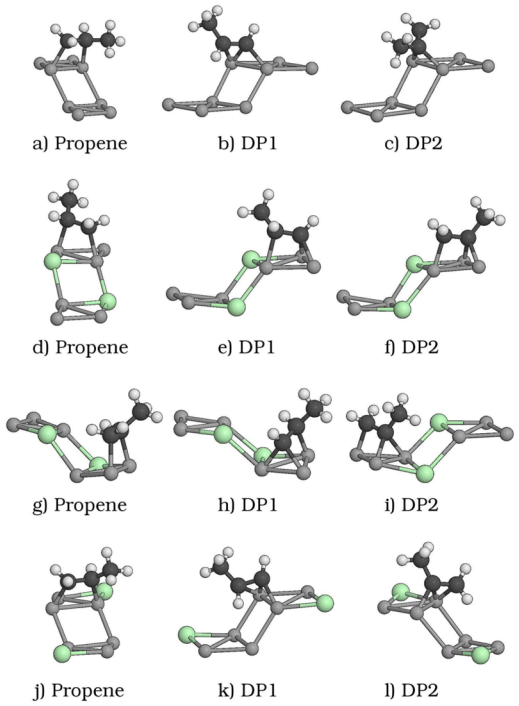

Figure 3. Adsorption geometries of propene and its dehydrogenation products (a-c) on Pt(211), (d-f) on di-σ_f and fcc sites of the α-step, (g-i) on di-σ_h and hcp sites of α-step, (j-i) and on the β-step. The spheres represent atoms, and they are colored such that H is white, Pt is light gray, C is dark gray, and Sn is light green.

Among the possible dehydrogenation processes, the highest activation energy is always found for dehydrogenation from the methyl group, which is consistent with an experimental observation that only three hydrogens of an adsorbed propene on Pt(111) can be exchanged with deuterium atoms.[12] The dehydrogenation reactions producing DP1 or DP2 are almost isoenergetic (see Table S4 in the SI), and the corresponding activation energies are 0.84 and 0.81 eV. They agree well with the calculated values reported in ref 17. The activation energies to form DP1 and DP2 are too close to each other to determine which one is preferred.

Compared with Pt(111), propene dehydrogenation on Pt(211) is more effective because the barrier drops to 0.54 eV for DP2 formation. This is somewhat higher than the value 0.29 eV reported earlier.[17] The activation energy of propene dehydrogenation on $Pt_3Sn(111)$ shows strong adsorption site dependence: Dehydrogenation from the di-σ_h (di-σ_f) site involves a barrier of 0.86 (1.31) eV. The large difference in activation energies originates from the large difference in adsorption energies of the final states. The correlation arises from the structural similarity of the transition state and product state geometries. The previously reported activation energy, 1.05 eV, for a di-σ_f site is lower than our value, probably again because of differences in the computational details.[21] On the α-

dx.doi.org/10.1021/cs400566y | ACS Catal. 2013, 3, 3026−3030

step, the dehydrogenation barriers are higher than on the flat $Pt_3Sn(111)$ surface. In contrast to Pt surfaces, where transition state geometries are very different (see Figure S3 in SI) and final products adsorb stronger on step sites, Pt_3Sn behaves differently. On the terrace and α-step of Pt_3Sn, the transition state geometries are very similar. Because they resemble final states, the activation energies correlate with the final state adsorption energies, which are weaker on the α-step than on the Pt_3Sn terrace, leading to higher activation energy at the α-step. The dehydrogenation barriers on the less stable β-step of Pt_3Sn, containing only Pt atoms, are nearly identical to those obtained on Pt(211); thus, the ligand effect, that is, changes in electronic properties due to the alloying with Sn, is minor.

On pristine catalyst particles, the concentration of β-steps is low owing to their higher surface energy, which makes them insignificant for dehydrogenation; however, they can possibly be formed by adsorbate-induced segregation either during the DHP reaction or in a regeneration process. This requires that an adsorbate have an adsorption energy of at least −0.93 eV to compensate for endothermic segregation. Thus, propene adsorption is not exothermic enough to do it. A Brønsted−Evans−Polanyi-like relation between the dehydrogenation activation energy and the adsorption energy of the final state (C_3H_5 + H) is observed on Pt(111), Pt(211), and $Pt_3Sn(111)$ (see Figure S5 in the SI). In general, the correlation is good. The activation energy of DP3 formation deviates from the general trend on Pt(111) and $Pt_3Sn(111)$ because the transition state geometry does not resemble the final state geometry. The observed poor correlation on the α-step, on the other hand, is due to a strong sterical hindrance of the species adsorbed at the hcp sites.

Experimental studies reporting propane dehydrogenation indicate that addition of hydrogen to the propane feed gas decreases coking.[6] We studied the effect of coadsorbed hydrogen on the adsorption and dehydrogenation of propene. At 0.25 ML coverage, the presence of a hydrogen atom on the Pt(111) surface decreases the adsorption energy of propene by 0.10 eV and increases the dehydrogenation barrier by 0.14 eV. We note that the changes are small but in the correct direction, indicating that even a single hydrogen atom impacts the process positively to reduce coking. However, the adsorption energy of a hydrogen atom is only −0.2 eV on a Pt(111) surface at 0.25 ML propene coverage. Therefore, a considerably higher hydrogen pressure is required for any hydrogen to be present on the surface at the reaction temperature.

DISCUSSION

Our calculations suggest that at low propene coverage, the step sites dominate the reactivity, leading to propene dehydrogenation, whereas at higher coverage, terrace sites are also populated, giving rise to molecular desorption. Calculations also show that on the flat surface, the activation energies are less affected by a change in surface activity due to the presence of Sn than the adsorption energies. In general, this increases the desorption rate compared with the dehydrogenation rate. Here, however, desorption is favored on both terraces because the transition state energies for dehydrogenation are above that of the gas-phase energy of propene, as shown by the potential energy surface (PES) in Figure 4. It is clear that propene dehydrogenation on Pt is dominated by steps because the barrier for dehydrogenation is smaller than for desorption. Computational findings may explain the low selectivity and subsequent rapid improvement for propane dehydrogenation

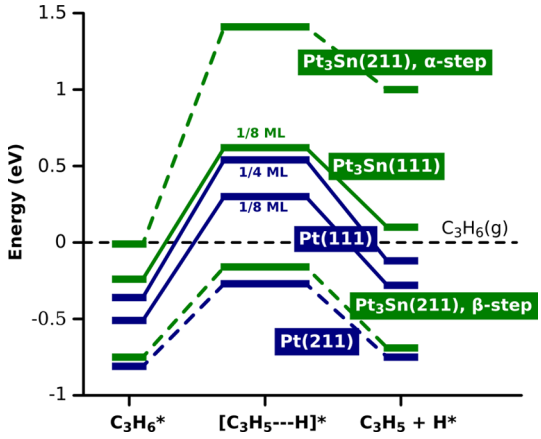

Figure 4. Potential energy surface of propene dehydrogenation. The lowest energy paths leading to DP1 or DP2 are presented.

on fresh Pt catalyst that are observed experimentally.[32] We tentatively ascribe the low initial selectivity to dehydrogenation and possible cracking of propene at the step sites. The selectivity improves after the steps are saturated by strongly adsorbed dehydrogenated species, reducing the rate of further bond-breaking reactions. On Pt_3Sn, the β-steps do dehydrogenate propene as readily as Pt steps, but a number of β-steps are small, whereas on α-steps and terraces, desorption is more favorable than dehydrogenation, as shown in the PES plot in Figure 4. Therefore, dehydrogenation on Pt_3Sn is less favorable than on Pt. This agrees very well with spectroscopic experiments, which show minor propene dehydrogenation on PtSn surface alloys.[7] The lack of very reactive Pt steps and more favorable desorption than dehydrogenation offers an explanation for the very high selectivity observed on Pt−Sn alloy catalysts, where Sn is also suggested to induce migration of coke precursors from the catalyst surface to the support.[5] The large difference in DHP selectivity observed on Pt and Pt−Sn catalysts[6] cannot be explained alone by the difference in propene dehydrogenation barrier heights on the (111) surfaces because they differ by only 0.3 eV. However, comparison of the smallest barriers on both surfaces, that is, on Pt(211) and Pt3Sn(111), shows a difference of 0.9 eV, which makes dehydrogenation on Pt_3Sn much less favorable than on Pt. The surface coverage can, in principle, affect the relative balance between the desorption and dehydrogenation rates. The PES shows that at higher (1/4 ML) coverage, the corresponding saturation coverage,[11] the propene binding is weaker, and the dehydrogenation barrier is higher than at lower, 1/8 ML, coverage. Thus, increased adsorbate coverage indicates higher selectivity.

To estimate the functional dependence of our results, we calculated non-self-consistent energies with the PBE[29] and the BEEF−vdW functional.[33] A PBE-calculated PES (not shown here) reproduces the majority of the features displayed in Figure 4 for the RPBE functional. The only difference is that on Pt(111), propene dehydrogenates rather than desorbs at low coverage, whereas desorption is preferred at high coverage. The BEEF−vdW functional includes van der Waals (vdW) interactions, unlike the RPBE and PBE functionals, and is also capable of describing chemisorption. Recent studies show that it performs excellently for the modeling of surface reactions.[34−36] For propene, BEEF−vdW adsorption energies become ∼0.3 eV more exothermic, and activation energies for dehydrogenation increase by ∼0.2 eV compared with the RPBE

dx.doi.org/10.1021/cs400566y | ACS Catal. 2013, 3, 3026−3030

values. Therefore, including the vdW interactions does not change our earlier conclusions based on RPBE results.

CONCLUSIONS

Our calculations demonstrate that by alloying Pt with Sn, we can control the number of reactive Pt step sites that can lead to improved selectivity via enhanced desorption compared with dehydrogenation. This can probably be achieved even with a small amount of Sn introduced on Pt catalysts because Sn atoms are known to decorate step sites.[16] The lack of reactive Pt steps on $Pt_3Sn(211)$ suppresses propene dehydrogenation, which explains in part the increased selectivity. In addition, the weaker propene adsorption identified here and in earlier studies[8,21] has a positive impact on the selectivity as propene desorption becomes easier. The experimentally observed diminished coking of Pt−Sn catalyst can be linked to reduced C−H bond breaking, and thus, decreased deep dehydrogenation, and weaker binding of propene and its derivatives,[6] facilitating their faster diffusion away from active sites.[5] The obtained results are not limited to propane dehydrogenation but have potential implications to all alkane dehydrogenation. The computational results call for experimental studies of the structure sensitivity of propene dehydrogenation on Pt and Pt−Sn alloys.

ASSOCIATED CONTENT

Supporting Information

Computational details, adsorption geometries, adsorption energies, and activation energies. This material is available free of charge via the Internet at http://pubs.acs.org.

AUTHOR INFORMATION

Corresponding Author

*E-mail: karoliina.honkala@jyu.fi.

Present Address

[†]Max-Planck-Institut für Eisenforschung GmbH, Department of Computational Materials Design, Max-Planck-Str. 1, D-40237 Düsseldorf, Germany.

Notes

The authors declare no competing financial interest.

ACKNOWLEDGMENTS

This work was financially supported by the Finnish Cultural Foundation and the Academy of Finland through Project 118532. The computational resources were provided by the Finnish IT Center for Science (CSC) Espoo.

REFERENCES

(1) Fessenden, R. J.; Fessenden, J. S. *Organic Chemistry*, 6th ed.; Brooks Cole: Belmont, CA, 1998.

(2) Bartholomew, C. H.; Farrauto, R. J. *Fundamentals of Industrial Catalytic Processes*, 2nd ed.; Wiley-Interscience: Hoboken, NJ, 2006.

(3) Bricker, J. C. *Top. Catal.* **2012**, *55*, 1309−1314.

(4) Kappenstein, C.; Guérin, M.; Lázár, K.; Matusek, K.; Paál, Z. *J. Chem. Soc., Faraday Trans.* **1998**, *94*, 2463−2473.

(5) Kumar, M. S.; Chen, D.; Holmen, A.; Walmsley, J. C. *Catal. Today* **2009**, *142*, 17−23.

(6) Bariås, O.; Holmen, A.; Blekkan, E. *J. Catal.* **1996**, *158*, 1−12.

(7) Tsai, Y.-L.; Xu, C.; Koel, B. E. *Surf. Sci.* **1997**, *385*, 37−59.

(8) Nykänen, L.; Honkala, K. *J. Phys. Chem. C* **2011**, *115*, 9578−9586.

(9) Panchenkov, G. M.; Kazanskaya, A. S.; Pershin, A. D. *Pet. Chem.* **1967**, *7*, 259−266.

(10) Cremer, P.; Su, X.; Shen, Y.; Somorjai, G. *J. Phys. Chem.* **1996**, *100*, 16302−16309.

(11) Zaera, F.; Chrysostomou, D. *Surf. Sci.* **2000**, *457*, 89−108.

(12) Salmeron, M.; Somorjai, G. A. *J. Phys. Chem.* **1982**, *86*, 341−350.

(13) Vang, R. T.; Honkala, K.; Dahl, S.; Schnadt, E. J.; Læsgaard, E.; Clausen, B. S.; Nørskov, J. K.; Besenbacher, F. *Nat. Mater.* **2005**, *4*, 160−162.

(14) Bus, E.; Ramaker, D.; van Bokhoven, J. *J. Am. Chem. Soc.* **2007**, *129*, 8094−8102.

(15) Andersin, J.; Lopez, N.; Honkala, K. *J. Phys. Chem. C* **2009**, *113*, 8278−8286.

(16) Virnovskaia, A.; Morandi, S.; Rytter, E.; Ghiotti, G.; Olsbye, U. *J. Phys. Chem. C* **2007**, *111*, 14732−14742.

(17) Yang, M.-L.; Zhu, Y.-A.; Fan, C.; Sui, Z.-J.; Chen, D.; Zhou, X.-G. *Phys. Chem. Chem. Phys.* **2011**, *13*, 3257−3267.

(18) Vajda, S.; Pellin, M. J.; Greeley, J. P.; Marshall, C. L.; Curtiss, L. A.; Ballentine, G. A.; Elam, J. W.; Catillon-Mucherie, S.; Redfern, P. C.; Mehmood, F.; Zapol, P. *Nat. Mater.* **2009**, *8*, 213−216.

(19) Segura, Y.; Lopez, N.; Perez-Ramirez, J. *J. Catal.* **2007**, *247*, 383−386.

(20) Studt, F.; Abild-Pedersen, F.; Bligaard, T.; Sørensen, R. Z.; Christiansen, C. H.; Nørskov, J. K. *Science* **2008**, *320*, 1320−1322.

(21) Yang, M.-L.; Zhu, Y.-A.; Zhou, X.-G.; Sui, Z.-J. *ACS Catal.* **2012**, *2*, 1247−1258.

(22) Valcárcel, A.; Ricart, J. M.; Clotet, A.; Illas, F.; Markovits, A.; Minot, C. *J. Catal.* **2006**, *241*, 115−122.

(23) Yang, M.-L.; Zhu, Y.-A.; Fan, C.; Sui, Z.-J.; Chen, D.; Zhou, X.-G. *J. Mol. Catal. A: Chem.* **2010**, *321*, 42−49.

(24) Enkovaara, J.; Rostgaard, C.; Mortensen, J. J.; Chen, J.; Dulak, M.; Ferrighi, L.; Gavnholt, J.; Glinsvad, C.; Haikola, V.; Hansen, H. A.; Kristoffersen, H. H.; Kuisma, M.; Larsen, A. H.; Lehtovaara, L.; Ljungberg, M.; Lopez-Acevedo, O.; Moses, P. G.; Ojanen, J.; Olsen, T.; Petzold, V.; Romero, N. A.; Stausholm, J.; Strange, M.; Tritsaris, G. A.; Vanin, M.; Walter, M.; Hammer, B.; Häkkinen, H.; Madsen, G. K. H.; Nieminen, R. M.; Nørskov, J. K.; Puska, M.; Rantala, T. T.; Schiøtz, J.; Thygesen, K. S.; Jacobsen, K. W. *J. Phys.: Condens. Matter* **2010**, *22*, 253202−24.

(25) Hammer, B.; Hansen, L. B.; Nørskov, J. K. *Phys. Rev. B* **1999**, *59*, 7413−7421.

(26) Gao, J.; Zhao, H.; Yang, X.; Koel, B. E.; Podkolzin, S. G. *ACS Catal.* **2013**, *3*, 1149−1153.

(27) Moll, N.; Kley, A.; Pehlke, E.; Scheffler, M. *Phys. Rev. B* **1996**, *54*, 8844−8855.

(28) Watwe, R.; Cortright, R.; Mavrikakis, M.; Nørskov, J.; Dumesic, J. *J. Chem. Phys.* **2001**, *114*, 4663−4668.

(29) Perdew, J. P.; Burke, K.; Ernzerhof, M. *Phys. Rev. B* **1996**, *77*, 3865−3868.

(30) Delbecq, F.; Sautet, P. *J. Catal.* **2003**, *220*, 115−126.

(31) Hammer, B.; Nørskov, J. K. *Adv. Catal.* **2000**, *45*, 71−129.

(32) Iglesias-Juez, A.; Beale, A.; Maaijen, K.; Weng, T.; Glatzel, P.; Weckhuysen, B. M. *J. Catal.* **2010**, *276*, 268−279.

(33) Wellendorff, J.; Lundgaard, K. T.; Møgelhøj, A.; Petzold, V.; Landis, D. D.; Nørskov, J. K.; Bligaard, T.; Jacobsen, K. W. *Phys. Rev. B* **2012**, *85*, 235149(23).

(34) Brogaard, R. Y.; Moses, P. G.; Nørskov, J. K. *Catal. Lett.* **2012**, *142*, 1057−1060.

(35) Studt, F.; Abild-Pedersen, F.; Varley, J. B.; Nørskov, J. K. *Catal. Lett.* **2013**, *143*, 71−73.

(36) Dell'Angela, M.; Anniyev, T.; Beye, M.; Coffee, R.; Föhlisch, A.; Gladh, J.; Katayama, T.; Kaya, S.; Krupin, O.; LaRue, J.; Møgelhøj, A.; Nordlund, D.; Nørskov, J. K.; Öberg, H.; Ogasawara, H.; Öström, H.; Pettersson, L. G. M.; Schlotter, W. F.; Sellberg, J. A.; Sorgenfrei, F.; Turner, J. J.; Wolf, M.; Wurth, W.; Nilsson, A. *Science* **2013**, *339*, 1302−1305.